

LLRF CONTROL AND SYNCHRONIZATION SYSTEM OF THE ARES FACILITY

S. Pfeiffer*, J. Branlard, F. Burkart, M. Hoffmann, T. Lamb, F. Ludwig, H. Schlarb, S. Schulz, B. Szczepanski, M. Titberidze, DESY, Hamburg, Germany

Abstract

The linear accelerator ARES (Accelerator Research Experiment at SINBAD) is a new research facility at DESY. Electron bunches with a maximum repetition rate of 50 Hz are accelerated up to 155 MeV. The facility aims for ultra-stable sub-femtosecond arrival-times and high peak-currents at the experiment, placing high demands on the reference distribution and field regulation of the S-band RF structures. In this paper, we report on the current status of the RF reference generation, facility-wide distribution, and the LLRF systems of the RF structures.

INTRODUCTION

The SINBAD (Short and Innovative Bunches and Accelerators at DESY) facility will host several accelerator research and development experiments [1]. The Accelerator Research Experiment at SINBAD (ARES) [2] is one of these experiments and will mainly focus on the production of low charge (0.5 pC to few pC) ultra-short (0.2 fs to 10 fs) electron bunches. ARES is a conventional S-band linear RF accelerator (linac) which is currently in the commissioning phase [3, 4]. It consists of S-band ($f_{RF} = 2.998$ GHz) normal conducting accelerating structures: one standing wave structure (1.5 cell RF-gun) and two traveling wave structures (TWS1, TWS2). The electron bunches are produced by impinging ultra-short laser pulses on a photo-cathode inside the RF-gun. An arrival time jitter of <10 fs rms is required to meet the final electron beam parameters at ARES. This puts high demands on the RF reference distribution to the accelerating structures and to the injector laser. This reference distribution is discussed in the following section. Furthermore, the LLRF systems for the RF structures are described and an example for the RF stability of the RF-gun is given. A short summary and an outlook on future steps conclude the paper.

RF SYNCHRONIZATION SYSTEM

The RF main oscillator (MO) is the heart of the RF synchronization system and generates the RF reference for all timing sensitive subsystems at the ARES facility. This RF reference signal is distributed via coaxial cables to various end stations. Furthermore, the injector laser is synchronized to the distributed RF reference. The current RF distribution is depicted in Fig. 1 and introduced in the following.

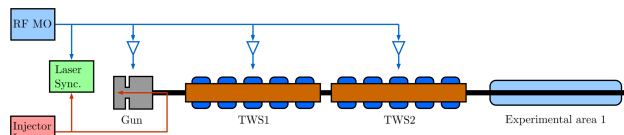


Figure 1: ARES layout - injector part up to the first experimental area.

Main Oscillator

The current MO is a commercial signal generator (R&S® SMA100B) delivering two RF signals. The main MO signal at 2.998 GHz is distributed throughout the ARES facility. A second, phase-locked signal at about 1 GHz (1/3 of the MO signal) is used as reference for the timing system [5]. A spectrally resolved phase noise measurement of the main MO signal is presented in Fig. 2.

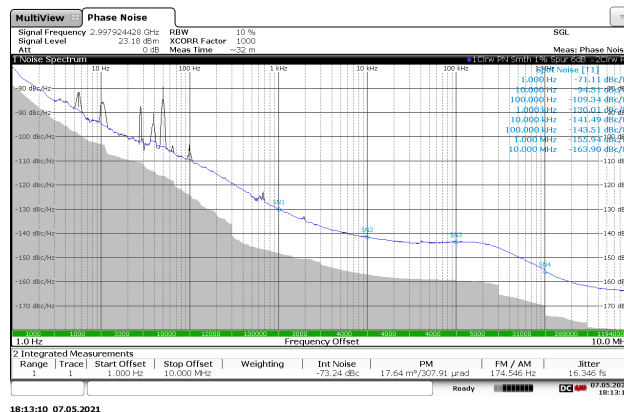


Figure 2: Noise characteristic of the SMA100B currently used as MO. The integrated phase noise amounts to 16.4 fs rms in the range [1 Hz ... 10 MHz].

The MO will be upgraded by the end of 2021 to improve the short and long term RF stability towards < 1 fs rms integrated jitter in the frequency range from 100 Hz to 10 MHz and an integrated jitter of < 10 fs rms from 1 Hz to 100 Hz. The MO is located in the injector area of the machine, next to the RF-gun and TWS1 racks, in order to keep the reference distribution distances to the critical end stations short. Two of these end stations, the injector laser and the accelerating structures are shortly explained in the following.

Laser Synchronization

In order to meet the challenging timing requirements it is crucial to achieve a precise synchronization between the pulsed injector laser and the 2.998 GHz RF reference signal from the MO. At present two synchronization schemes

* sven.pfeiffer@desy.de

Content from this work may be used under the terms of the CC BY 3.0 licence (© 2021). Any distribution of this work must maintain attribution to the author(s), title of the work, publisher, and DOI

have been studied and implemented [6, 7]. The direct synchronization based synchronization setup is in permanent (24/7) operation and the measured in-loop timing jitter of the injector laser amounts to about 18 fs rms from 10 Hz to 186 kHz. This performance is sufficient for the initial phase of the experiments planned at ARES. However, lately an additional synchronization scheme based on a Mach-Zehnder modulator (MZM) has been implemented which exhibits significant lower excess jitter and phase drift.

Accelerating Structure Synchronization

In each LLRF rack, the 2.998 GHz RF reference signal is connected to a reference module (REFM), where it is amplified and distributed to the different sub-modules in this rack. The idea of the REFM is to actively compensate RF drifts using an RF interferometer to measure and control the RF phase of the RF reference. Additional RF signals are locally generated by an universal local oscillator generation module (uniLOGM). It internally divides and mixes the RF reference signal to produce the local oscillator signal (LO) for the down-converters and the clock signal (CLK) for the digitizers.

LLRF SYSTEM

The LLRF systems for the RF-gun and TWS1 are housed in one rack, next to the MO rack. A second rack is used for the TWS2 LLRF system. The RF reference signal is distributed in the shortest possible way from the MO to the two LLRF racks. The temperature stabilized racks for the LLRF systems and the MO rack are located in the basement underneath the accelerator tunnel to keep the cables for the signal detection short. By installing the racks in the basement, we expect fewer RF drifts in the acquisition chain due to the partial decoupling from external environmental disturbances. Each rack contains additional support modules such as a power supply module (PSM) and the universal local oscillator generation module (uniLOGM). In addition, a drift compensation module (DCM) is installed in the rack to locally reduce the effects of humidity and temperature on the RF signal detection cables [8]. The rack layout is depicted in Fig. 3.

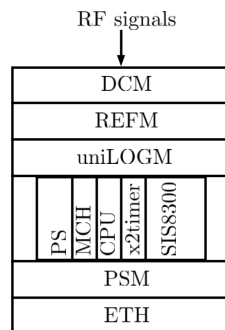


Figure 3: Exemplary LLRF rack layout.

The LLRF system for the RF-gun, TWS1 and TWS2 regulation is based on MicroTCA.4 technology very similar to

the single cavity LLRF system e.g. used at the REGAE facility [9]. Each MicroTCA crate of the LLRF system consists of a power supply (PS), a MicroTCA Carrier Hub (MCH), a CPU, a timing module and one or more ADC (SIS8300-L2) and down-converter/vector-modulator boards (DWC8VM1). A sampling and processing frequency of 125 MHz has been chosen. The drive RF pulse length for the RF structures is limited by the modulator pulse length of up to 6 μ s at the current RF pulse repetition rate of 10 Hz. A pre-amplifier, located in a separate rack near the klystron/modulator drives the klystron and closes the control loop to the cavity. The detection of the full RF pulse including decay requires 2048 sampling points recorded and stored in a data acquisition (DAQ) system.

RF-Gun

The LLRF system for the RF-gun receives RF signals from various points along the low level signal path, i.e. the RF reference, the vector-modulator output and the pre-amplifier output signals as well as from the high power signal chain the forward and reflected signals from/to the klystron and the signal from the RF probe installed in the full RF cell (see Fig. 4).

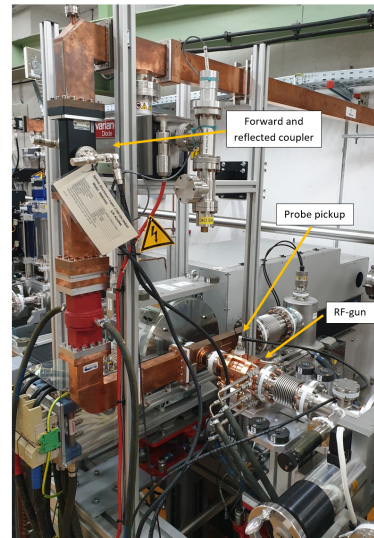


Figure 4: RF-gun system with signals detected at the directional coupler, in the waveguide distribution and via the RF-probe.

The recorded signals allow stability check for the drive signals along the signal chain shortly outlined in the following. The signals have been optimized to 83% ADC range at the highest expected operating gradient. At the current operating gradient of 70MV/m expected field at the cathode, the ADC operating point is at 63%. The signal traces have been recorded and analyzed at the beam position, see Fig. 5. This analysis has been performed as average of 51 sampling points in a time span $t_{beam} \pm 200$ ns. The signal to noise ratio increases by reducing the expected noise bandwidth to 2.45 MHz which is still a factor 10 higher than the RF-gun bandwidth of about 244 kHz [10]. Slow drifts which are

correctable are taken out using a polynomial function, restricting the result to the remaining fast variations as shown in Fig. 6. With the current setup and an active pulse to pulse adaptation we achieve an amplitude and phase stability of 0.013% and 0.016 deg for the RF probe signal. We did not observe larger noise contributions along the RF chain from the vector-modulator to the probe signal.

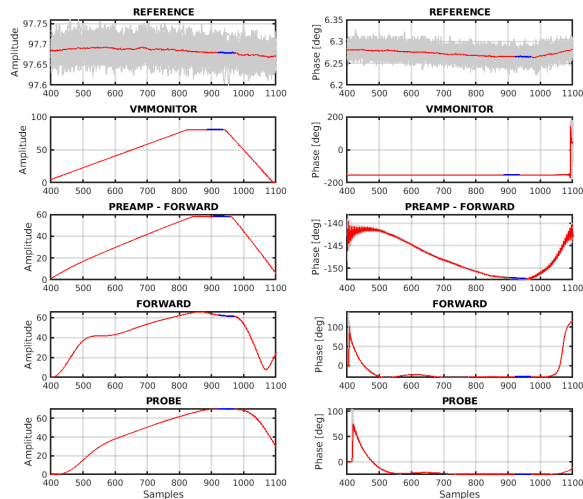


Figure 5: Signal in amplitude and phase for detected drive signals. The blue area depicts the sampling points for averaging. The reference signal from the REFEM is connected to one dedicated channel, yielding the expected ADC resolution and noise contribution.

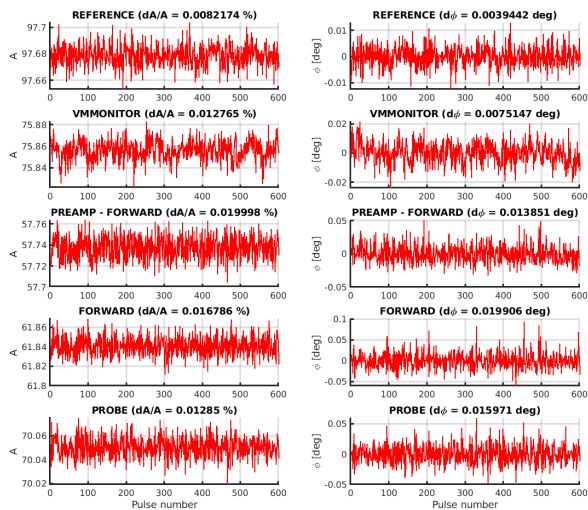


Figure 6: Pulse to pulse variations of the signals at beam position.

TWS1 and TWS2

The LLRF systems for TWS1 and TWS2 receive signals similar to the RF-gun system. However, 5 additional probe pickups are installed, one at the beginning, one at the end of the structure and 3 evenly distributed between the solenoids,

Fig. 7. The goal for 5 probe signals along with 4 temperature sensors between the RF pickups is to precisely estimate the temperature profile used for RF and temperature regulation. In addition, efforts are being made to regulate the expected energy gain by combining the 5 probe signals for LLRF control. This is currently being investigated at the ARES facility.

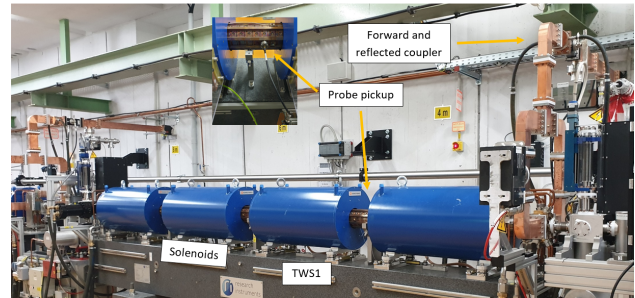


Figure 7: TWS1 system with the forward and backward wave signal acquisition at the directional coupler and as an example one probe pickup (from a total of five).

CONCLUSION AND NEXT STEPS

In this paper we introduced the LLRF system for the ARES RF structures. The system for the RF-gun and the two traveling wave structures are in operation 24/7. The signals have been calibrated with beam based on spectrometer measurements and the RF simulation. Furthermore, the ADC and DAC signals have been optimized on the digital level. A performance evaluation exemplary shown for the RF-gun did not show larger noise sources along the signal chain. The passive RF distribution and the direct laser to RF synchronization is currently sufficient for first commissioning. First long term beam based stability measurements using a spectrometer after the last TWS did not show larger RF drifts.

At the end of 2021 we plan to upgrade the MO to further reduce amplitude and phase noise. The LLRF system for the two new Polari-X structures [11] operating at X-band ($f_{RF} = 12$ GHz) will be installed soon. This system requires up and down conversion modules from/to 3 GHz to/from 12 GHz, which have been developed and measured. Initial intra-pulse feedback tests for the RF-gun show improvements in the probe regulation by a factor of 1.5 for the RF phase. Learning the optimal intra-pulse setpoint trajectory is required to bring this feedback scheme into continuous operation. The optimal RF regulation for the TWS, with 1 or 5 probes as regulation signal, is under investigation. An upgrade of the REFEMs for interferometric transmission line stabilization is being planned to improve the RF synchronization.

ACKNOWLEDGMENT

The authors acknowledge support from DESY (Hamburg, Germany), a member of the Helmholtz Association HGF.

REFERENCES

- [1] B. Marchetti *et al.*, “Electron-Beam Manipulation Techniques in the SINBAD Linac for External Injection in Plasma Wake-Field Acceleration”, *Nuclear Instruments and Methods in Physics Research Section A: Accelerators, Spectrometers, Detectors and Associated Equipment*, vol. 829, pp. 278–283, Sep. 2016. doi:10.1016/j.nima.2016.03.041
- [2] B. Marchetti *et al.*, “Technical Design Considerations About the SINBAD-ARES Linac”, in *Proc. 7th Int. Particle Accelerator Conf. (IPAC’16)*, Busan, Korea, May 2016, pp. 112-114. doi:10.18429/JACoW-IPAC2016-MOPMB015
- [3] B. Marchetti *et al.*, “Status of the ARES RF Gun at SINBAD: From its Characterization and Installation towards Commissioning”, in *Proc. 9th Int. Particle Accelerator Conf. (IPAC’18)*, Vancouver, Canada, Apr.-May 2018, pp. 1474-1476. doi:10.18429/JACoW-IPAC2018-TUPMF086
- [4] E. Panofski *et al.*, “Status Report of the SINBAD-ARES RF Photoinjector and LINAC Commissioning”, in *Proc. 10th Int. Particle Accelerator Conf. (IPAC’19)*, Melbourne, Australia, May 2019, pp. 906-909. doi:10.18429/JACoW-IPAC2019-MOPTS026
- [5] A. Hidvégi, P. Geßler, H. Kay, K. Rehlich, and C. Bohm, “Timing and Triggering System for the European XFEL Project - a Double Sized AMC Board”, in *Proc. 18th IEEE-NPSS Real Time Conference*, Berkeley, CA, USA, Jun. 2012, paper PS4-12, p. 777.
- [6] M. Titberidze *et al.*, “First results on Femtosecond Level Photocathode Laser Synchronization at the SINBAD Facility”, in *Proc. 8th Int. Beam Instrumentation Conf. (IBIC’19)*, Malmö, Sweden, Sep. 2019, pp. 564-567. doi:10.18429/JACoW-IBIC2019-WEPP020
- [7] M. Titberidze *et al.*, “Precise Laser-to-RF Synchronization of Photocathode Lasers”, in *Proc. 39th Int. Free Electron Laser Conf. (FEL’19)*, Hamburg, Germany, Aug. 2019, pp. 364-367. doi:10.18429/JACoW-FEL2019-WEP016
- [8] C. Schmidt *et al.*, “Operational Experience of the Drift Compensation Module at the European XFEL and FLASH”, presented at the Low-Level Radio Frequency Workshop (LLRF19), Chicago, IL, USA, Sep.-Oct. 2019, unpublished.
- [9] M. Hoffmann *et al.*, “High Speed Digital LLRF Feedbacks for Normal Conducting Cavity Operation”, in *Proc. 5th Int. Particle Accelerator Conf. (IPAC’14)*, Dresden, Germany, Jun. 2014, pp. 2430-2432. doi:10.18429/JACoW-IPAC2014-WEPME066
- [10] S. Pfeiffer, J. Branlard, F. Burkart, M. Hoffmann, and H. Schlarb, “Parameter Estimation of Short Pulse Normal-Conducting Standing Wave Cavities”, presented at the 12th Int. Particle Accelerator Conf. (IPAC’21), Campinas, Brazil, May 2021, paper WEPAB295, this conference.
- [11] P. Craievich *et al.*, “Novel X-band transverse deflection structure with variable polarization”, *Physical Review Accelerators and Beams*, vol. 23, p. 112001, Nov. 2020. doi:10.1103/PhysRevAccelBeams.23.112001